Organic Process Research & Development **2010**, *14*, 1304–1312

A Kinetic and Mass Transfer Model for Glycerol Hydrogenolysis in a Trickle-Bed Reactor

Yaoyan Xi,[†] Jonathan E. Holladay,[§] John G. Frye,[§] Aaron A. Oberg,[†] James E. Jackson,[‡] and Dennis J. Miller*[,†]

Department of Chemical Engineering and Materials Science, Michigan State University, East Lansing, Michigan 48824, U.S.A., and Department of Chemistry, Michigan State University, East Lansing, Michigan 48824, U.S.A., and Pacific Northwest National Laboratory, PO Box 999, Richland, Washington 99352, U.S.A.

Abstract:

A detailed model of glycerol hydrogenolysis in a trickle-bed reactor is presented that includes a mechanistically based kinetic rate expression, energy transport, mass transport across the gas−liquid and liquid−solid interfaces, intraparticle catalyst mass transfer, and partial wetting of the bed. Optimal kinetic parameters for the glycerol hydrogenolysis rate expression were determined via nonlinear regression analysis on the basis of experiments conducted in a laboratory-scale trickle-bed reactor over a broad range of operating conditions. Model predictions agree well with experimental data and accurately predict trends in reactor performance with liquid flow rate, temperature, hydrogen pressure, and base promoter concentration. The model is thus a useful tool for predicting laboratory reactor performance and for design of commercial-scale trickle-bed systems.

Introduction

Glycerol (1,2,3-propanetriol, herein GO) has become an attractive feedstock for chemicals production because it is readily available as the major byproduct from biodiesel production.[1] In particular, GO hydrogenolysis to propylene glycol (PG) has received attention in both patent and open literature, because PG is a thousand kilo-tonne commodity with applications as a polymer building block, emollient in consumer products, and nontoxic replacement for ethylene glycol (EG).

Among numerous patents describing GO conversion to PG, Casale et al.[1] used sulfide-modified ruthenium to achieve 75% PG yield; Schuster et al.[2] used a mixed metal (Cu/Co/Mn/Mo) catalyst with heteropolyacids that gave 96% PG yield, and Werpy et al.[3] demonstrated >80% selectivity to PG over a Ni/Re catalyst.

The open literature contains several studies of catalysts for PG formation from GO, including bimetallic Pt/Ru and Au/Ru catalysts at neutral and elevated pH,[4] carbon-supported Ru and Pt,[5] Amberlyst ion-exchange resins in conjunction with Ru/C,[6] Cu/ZnO unsupported materials with different domain sizes and metal content ratios,[7] cobalt nanowires,[8] and others.[9] In mechanistic studies, Feng et al.[10] describe the role of support and Ru catalyst reduction temperature, and Shanks et al.[11] investigate competitive adsorption of several polyol species on Ru. Mechanisms have been proposed for several catalyst systems: Kovacs et al.[12] for base-promoted metal catalysis involving glyceraldehyde and pyruvaldehyde intermediates; Hass et al.[13] for solid acid catalysts via an acrolein intermediate, and Suppes et al.[14] via GO dehydration and hydrogenation via acetol as the intermediate.

Glycerol hydrogenolysis is a three-phase reaction system typically involving solid catalyst, liquid solution of reactants and products, and gaseous hydrogen. Although most laboratory studies are carried out in batch autoclaves, three-phase continuous reactors, in particular trickle-bed systems, are preferred for large-scale, commercial applications.[15−19] Trickle-bed reactors are widely employed in hydrotreating processes such as hydrogenolysis, hydrodesulfurization, hydrocracking and hydrorefining.

The characterization of mass and heat transfer in trickle-bed reactors, particularly at the gas−liquid (G−L) interface, has been widely studied.[16,20−23] Al-Dahhan et al.[16] set forth a quantitative model taking into account flow regime transitions, liquid holdup, pressure drop, gas−liquid interfacial area, and catalyst wetting efficiency in both liquid-limited and gas-limited

* Corresponding author. E-mail: millerd@egr.msu.edu.
† Department of Chemical Engineering and Materials Science, Michigan State University.
‡ Department of Chemistry, Michigan State University.
§ Pacific Northwest National Laboratory.

(1) Casale, B., Gomez, A. Method of Hydrogenating Glycerol. U.S. Patent 5,214,219, 1993) (CAS #118:168689).
(2) Schuster, L.; Eggersdorfer, M. Preparation of 1,2-Propanediol. U.S. Patent 5,616,817, 1997 (CAS #125:57901).
(3) Werpy, T. A.; Frye, J. G.; Zacher, A. H.; Miller, D. J. Hydrogenolysis of 6-Carbon Sugars and Other Organic Compounds. U.S. Patent 6,841,085, 2005 (CAS #138:339970).
(4) Maris, E. P.; Ketchie, W. C.; Murayama, M.; Davis, R. J. *J. Catal.* **2007**, *251*, 281–294.
(5) Maris, E. P.; Davis, R. J. *J. Catal.* **2007**, *249*, 328–337.
(6) Miyazawa, T.; Koso, S.; Kunimori, K.; Tomishige, K. *Appl. Catal. A* **2007**, *329*, 30–35.
(7) Wang, S.; Liu, H. *Catal. Lett.* **2007**, *117*, 62–67.
(8) Liu, Q.; Guo, X.; Chen, J. L.; Li, J.; Song, W.; Shen, W. *J. Nanotechnology* **2008**, *19*, 1–9.
(9) Huang, L.; Zhu, Y.; Zheng, H.; Li, Y.; Zeng, Z. *J. Chem. Technol. Biotechnol.* **2008**, *83*, 1670–1675.
(10) Feng, J.; Fu, H.; Wang, J.; Li, R.; Chen, H.; Li, X. *Catal. Commun.* **2008**, *9*, 1458–1464.
(11) Shanks, B. H.; Lahr, D. G. *Ind. Eng. Chem. Res.* **2003**, *42*, 5467–5472.
(12) Kovacs, D. G.; Jackson, J. E.; Miller, D. J. *Proceedings of the 219th American Chemical Society Meeting*; American Chemical Society: Washington, DC, 2000.
(13) Hass, T.; Neher, Armin, Arntz, D.; Klenk, H.; Girke, W. *Process for the Simultaneous Production of 1,2- and 1,3-Propanediol*. U.S. Patent 5,426,249, 1995 (CAS #121: 82510).
(14) Dasari, M. A.; Kiatsimkul, P.; Sutterlin, W. R.; Suppes, G. *J. Appl. Catal. A* **2005**, *281*, 225–231.
(15) Dudukovic, M. P.; Larachi, F.; Mills, P. L. *Chem. Eng. Sci.* **1999**, *54*, 1975–1995.
(16) Al-Dahhan, M. H.; Larachi, F.; Dudukovic, M. P.; Laurent, A. *Ind. Eng. Chem. Res.* **1997**, *36*, 3292–3314.
(17) Dudukovic, M. P. *Catal. Today* **1999**, *48*, 5–15.
(18) Biardi, G.; Baldi, G. *Catal. Today* **1999**, *52*, 223–234.
(19) Gianetto, A.; Specchia, V. *Chem. Eng. Sci.* **1992**, *47*, 3197–3213.

Published on Web 10/01/2010
10.1021/op900336a

scenarios. Larachi et al.[20] proposed a rigorous model for G−L mass transfer at elevated pressure that accounts for liquid and gas nonidealities along with pressure, gas and liquid superficial velocities, liquid viscosity, and packing size. Iliuta et al.[21] studied the fluid dynamics along with G−L mass transfer, and Huang et al.[22] studied heat transfer in detail. A correlation for catalyst wetting efficiency in elevated pressure trickle-bed reactors was developed by Al-Dahhan[23] to correlate laboratory- and pilot-scale data.

Trickle-bed models that include the above phenomena have successfully predicted reactor performance in a number of pilot-scale and commercial systems. These include, among others, carbohydrate hydrogenolysis,[24] benzene hydrogenation,[25] catalytic oil hydrotreating,[26] dicyclopentadiene hydrogenation,[27] phenol oxidation,[28,29] 1,5,9-cyclododecatriene,[30] phenylacetylene,[31] and 2,4-dinitrotoluene.[32] In all of these studies, partial wetting of the catalyst, gas−liquid and liquid−solid mass transport, and reaction kinetics were incorporated to provide successful descriptions of the reactor behavior.

In this contribution, we present experimental and modeling studies of GO hydrogenolysis in a trickle-bed reactor. GO is both a commercially important feedstock and a model carbohydrate, and its hydrogenolysis to PG represents a reaction that will be commonly carried out in the emerging biorefinery. The effect of mass transfer between the gas, solid, and liquid phases, partial wetting of the catalyst bed, intrinsic reaction kinetics, and process operating conditions on GO conversion are presented and discussed.

Experimental Section

Materials. Ultrahigh purity gases used in experiments—hydrogen (99.999%), nitrogen (99.99%), helium (99.999%), and oxygen (99.99%)—were obtained from Linde Gas LLC. Anhydrous glycerol (99.9%), sodium hydroxide pellets (98.7%), lactic acid (88.9%), and water (99.99%) were purchased from J.T. Baker. Propylene glycol (99.5%) was obtained from Jade Scientific, Inc.; ethylene glycol (99.0%) was produced by Spectrum, Inc., and sulfuric acid (98%) was purchased from Columbus Chemical Industries, Inc.

(20) Larachi, F.; Cassanello, M.; Laurent, A. *Ind. Eng. Chem. Res.* **1998**, *37*, 718–733.
(21) Iliuta, I.; Ortiz-Arroyo, A.; Larachi, F.; Grandjean, B. P. A.; Wild, G. *Chem. Eng. Sci.* **1999**, *54*, 5329–5337.
(22) Huang, X.; Varma, A.; McCready, M. J. *Chem. Eng. Sci.* **2004**, *59*, 3767–3776.
(23) Al-Dahhan, M. H.; Dudukovic, M. P. *Chem. Eng. Sci.* **1995**, *50*, 2377–2389.
(24) Tronconi, E.; Ferlazzo, N.; Forzatti, P.; Pasquon, I.; Casale, B.; Marini, L. *Chem. Eng. Sci.* **1992**, *47*, 2451–2456.
(25) Roininen, J.; Alopaeus, V.; Toppinen, S.; Aittamaa, J. *Ind. Eng. Chem. Res.* **2009**, *48*, 1866–1872.
(26) Mederos, F. S.; Rodriguez, M. A.; Ancheyta, J.; Arce, E. *Energy Fuel* **2006**, *20*, 936–945.
(27) Liu, G.; Mi, Z.; Wang, L.; Zhang, X.; Zhang, S. *Ind. Eng. Chem. Res.* **2006**, *45*, 8807–8814.
(28) Suwanprasop, S.; Eftaxias, A.; Stuber, F.; Polaert, I.; Julcour-Lebigue, C.; Delmas, H. *Ind. Eng. Chem. Res.* **2005**, *44*, 9513–9523.
(29) Guo, J.; Al-Dahhan, M. *Ind. Eng. Chem. Res.* **2005**, *44*, 6634–6642.
(30) Dietz, A.; Julcour, C.; Wilhelm, A. M.; Delmas, H. *Catal. Today* **2003**, *79*, 293–305.
(31) Huang, X.; Wilhite, B.; McCready, M. J.; Varma, A. *Chem. Eng. Sci.* **2003**, *58*, 3465–3471.
(32) Rajashekharam, M. V.; Jaganathan, R.; Chaudhari, R. V. *Chem. Eng. Sci.* **1998**, *53*, 787–805.

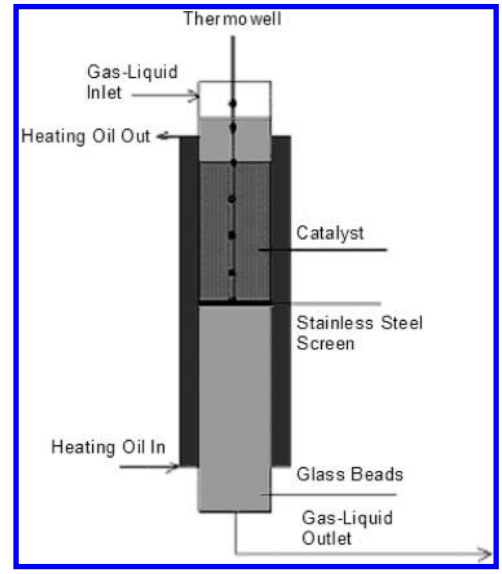

Figure 1. **Laboratory trickle-bed reactor.**

The catalyst used in this study is composed of 2.5 wt % Co, 0.5 wt % Pd, and 2.4 wt % Re supported on a proprietary activated carbon. The catalyst was prepared by incipient wetness of a nitrate salt solution of the metals, followed by slow drying and calcination in inert gas. The catalyst was reduced in pure hydrogen (100 cm^3 (STP)/min) using a temperature ramp of 1.5 °C/min to 350 °C and then holding at 350 °C for two hours. Hydrogen chemisorption was performed on the catalyst at 308 K in a Micromeritics ASAP 2010 volumetric adsorption apparatus; the sample was outgassed at 623 K prior to adsorption. A catalyst site density of 1.3×10^{-5} kmol/kg catalyst, corresponding to a catalyst metal dispersion of ~2.5%, was measured as the difference between the quantities of total and weakly adsorbed hydrogen. The final supported catalyst has a nitrogen BET surface area of 840 ± 20 m^2/g and a bulk density in the trickle bed of approximately 700 kg/m^3.

Trickle-Bed Reactor. All experimental GO hydrogenolysis data were collected in a 40 cm^3 laboratory trickle-bed reactor of dimensions 1.25 cm i.d. and 61 cm in length (Figure 1) loaded with the aforementioned carbon-supported metal catalyst. The catalyst (27 cm depth, 24.0 g) was placed between a 10 cm layer of 2 mm diameter glass beads at the bottom of the bed and a 15 cm layer of 2 mm diameter stainless steel beads at the top of the bed to facilitate liquid distribution and preheating prior to reaction. Prior to reaction, the catalyst was re-reduced in situ with pure hydrogen flowing at 100 cm^3 (STP/min) at 280 °C for at least 2 hours. An Isco 500-mL syringe pump was used to introduce liquid feed solution into the reactor, and a Porter LB366 mass flow controller was used to control helium and hydrogen gas flow rates. The catalyst bed, located in the center of the reactor, was heated by a recirculating silicon oil (Dynalene 6000) stream flowing through a jacket surrounding the reactor and controlled by a Julabo SE-6 programmable recirculating bath. A chromel−alumel thermocouple located in a thermowell along the center axis of the bed was used to measure the trickle-bed temperature profile during reaction.

Experiments were carried out using a 40 wt % (4.6 M) GO feed solution with sodium hydroxide (0.1−0.6 M) as a base promoter. Hydrogen was fed to the reactor at a rate correspond-

ing to a 5:1 H_2:GO molar ratio for all experiments. Pressure (3.3−13.3 MPa), temperature (453−475 K), and feed flow rate (25−50 mL/h) were varied to characterize catalyst and reactor performance. During reaction, liquid product samples were collected for 5 min every hour; the liquid collected during the time between samples was retained in a large storage tank.

All liquid samples were analyzed with a Waters high performance liquid chromatography system with a Waters 717 Plus autosampler and a BioRAD Aminex HPX-87H column (7.8 mm ×300 mm) with 5 mM H_2SO_4 as the mobile phase at a flow rate of 0.55 mL/min; a Waters 2414 refractive index (RI) detector was used in the HPLC to measure liquid sample concentrations. The RI detector was calibrated via a multipoint calibration curve for all reaction species.

Kinetic Model for Glycerol Hydrogenolysis

The establishment of the reactor model begins with development of a kinetic rate expression based on our previously proposed reaction mechanism for GO hydrogenolysis over supported metal catalysts.[12] In simplified form, the mechanism involves (1) dehydrogenation of GO to an adsorbed glyceraldehyde analogue (GA·S), (2) rearrangement and dehydration of GA·S to a second adsorbed intermediate (I·S) analogous to pyruvaldehyde, and (3) hydrogenation of the second intermediate to propylene glycol (PG).

$$\mathrm{GO} + \mathrm{S} \underset{k_{-1}}{\overset{k_1}{\rightleftharpoons}} \mathrm{GA{\cdot}S} + H_2 \tag{1}$$

$$\mathrm{GA{\cdot}S} + \mathrm{OH^-} \underset{k_{-2}}{\overset{k_2}{\rightleftharpoons}} \mathrm{I{\cdot}S} + \mathrm{OH^-} \tag{2}$$

$$\mathrm{I{\cdot}S} + 2\mathrm{H_2} \xrightarrow{k_3} \mathrm{PG} + \mathrm{S} \tag{3}$$

The rate expression for each step shown above can be written as follows:

$$r_1 = k_1 C_{\mathrm{GO}} \cdot C_{\mathrm{S}} - k_{-1} C_{\mathrm{GA{\cdot}S}} C_{\mathrm{H_2}} \tag{4}$$

$$r_2 = k_2 C_{\mathrm{GA{\cdot}S}} C_{\mathrm{OH^-}} - k_{-2} C_{\mathrm{I{\cdot}S}} C_{\mathrm{OH^-}} \tag{5}$$

$$r_3 = k_3 C_{\mathrm{I{\cdot}S}} C_{\mathrm{H_2}}^2 \tag{6}$$

Equating the three rates, invoking the site balance,

$$C_{\mathrm{total}} = C_{\mathrm{S}} + C_{\mathrm{GA{\cdot}S}} + C_{\mathrm{I{\cdot}S}} \tag{7}$$

and eliminating the concentrations of adsorbed intermediates gives a final, complete rate expression from the mechanism (see Supporting Information). In order to further simplify the rate expression, three terms in the denominator of the final rate expression were eliminated because they added no additional features to the expression and they introduced additional kinetic parameters. The final, simplified rate expression is given below as eq 8.

$$r_1 = \frac{k_{\mathrm{f}} C_{\mathrm{GO}} C_{\mathrm{OH^-}} C_{\mathrm{H_2}}^2}{C_{\mathrm{GO}} C_{\mathrm{OH^-}} + K_{\mathrm{H}} C_{\mathrm{H_2}}^3} \tag{8}$$

In this model, GO hydrogenolysis kinetics are thus described in terms of only three parameters: a pre-exponential factor k_0 and activation energy E_a in k_f, and an adsorption constant K_H taken as independent of temperature. This rate expression captures essential features observed in GO hydrogenolysis: fractional reaction order with respect to GO and hydroxide promoter, and positive-to-negative reaction order with respect to hydrogen as hydrogen pressure increases.

The rate expression derived for GO hydrogenolysis does not contain any information about selectivity to products, even though historically methane, ethylene glycol, and lactic acid are noted as byproducts of GO hydrogenolysis to PG. In this study, the catalyst showed selectivities to PG between 88 and 95% of theoretical over the range of operating conditions, with byproducts ethylene glycol (2−3%), lactic acid (1−3%), and alcohols (methanol, ethanol, propanol) (1.5−3.5%) consuming the remainder of GO. To include formation of these byproducts explicitly in this model would require an additional rate expression for each species; such additional complexity is not warranted because byproduct yields are relatively constant and it would be extremely difficult to obtain distinct rate expressions for byproduct formation from solely the outlet concentrations of those species.

Trickle-Bed Reactor Model

Balance Equations. The trickle-bed model for GO hydrogenolysis is developed for steady-state operation by assuming one-dimensional plug flow for the liquid phase.[33] The molar balance for GO is thus given by

$$-\frac{\mathrm{d}C_{\mathrm{GO}}}{\mathrm{d}\tau} = R_{\mathrm{G}} \tag{9}$$

where τ is defined as reactor volume divided by liquid flow rate.

For GO hydrogenolysis in the trickle bed, it is not necessary to write a molar balance for the gas phase. The significant molar excess of hydrogen used in reactions (5:1 H_2/GO) and the formation of negligible quantities of gas-phase products (less than 1% of GO is converted to methane) means that the gas phase is essentially composed of hydrogen and water at its vapor pressure over the reacting solution. Thus, gas composition does not change down the length of the trickle bed. Further, the high gas-phase pressure (3−12 MPa) results in very small gas superficial velocities through the reactor (<10 cm/min) and thus low pressure drop (<10 kPa), and thus gas phase has essentially no influence on liquid flow in the trickle bed.

The energy balance includes terms for heat generation by reaction and energy removal by the coolant surrounding the reactor.

$$\frac{\mathrm{d}(\rho C_{\mathrm{p}} T)}{\mathrm{d}\tau} = (-\Delta H_{\mathrm{R}})(-R_{\mathrm{G}}) + \frac{2U_0}{R}(T_{\mathrm{c}} - T) \tag{10}$$

(33) Levenspiel, O. *Chemical Reaction Engineering*, 3rd ed.; John Wiley & Sons: New York, 1999.
(34) Smith, J. M. *Chemical Engineering Kinetics*, 3rd ed.; McGraw-Hill: New York, 1981.

The overall heat transfer coefficient (U_o) between the catalyst bed and coolant was taken as 250 J/m^2/s/K;[34] varying this value by ±20% led to larger variations between predicted and experimental temperature profiles in the trickle bed, and thus this value was used for all simulations. The jacket temperature (T_c) used in the reactor model was taken as the recirculating oil bath set-point temperature.

It is worth noting that temperature changes in the trickle bed should be dampened by the phase equilibrium between the liquid and gas phases. Energy liberated by reaction raises the liquid phase temperature, but that rise in temperature is offset by the corresponding increase in water vapor pressure which forces the energy liberated in reaction to produce more water vapor to re-establish equilibrium. Thus, for a constant water mole fraction in the liquid phase and negligible pressure drop in the reactor, the reactor temperature should be approximately constant.

Mass Transfer Relationships. In order to properly determine the global reaction rate (R_G) in the trickle bed, gas−liquid and liquid−solid interphase mass transfer of H_2, liquid−solid mass transfer of GO, and intraparticle mass transport of H_2 and GO in the catalyst must be considered. The hydrogen mass transfer coefficients $k_{GL,H_2}a$ and $k_{LS,H_2}a$ were taken from the trickle-bed correlations of Goto and Smith;[35] values for the coefficients vary with conditions but are approximately 0.02/s and 0.1/s, respectively.

Within the catalyst particles, hydrogen is the limiting reactant because its concentration (e.g., solubility) in water at the pressures used in this study is low (0.03−0.1 M) compared to that of GO (0.5−4.8 M). Even though the liquid-phase diffusivity of GO is only about one-fifth that of hydrogen, GO concentration gradients relative to those of hydrogen within the catalyst particles and between bulk liquid and solid can be neglected—an assumption that is valid except perhaps where GO is nearly fully consumed in the bed, in which case reaction rates are low and intraparticle diffusion is unimportant anyway.

The effective diffusivity of hydrogen in catalyst particles is estimated via the random pore model ($D_{e,H_2} = D_{H_2} \cdot \varepsilon_p^2$), where the particle porosity (ε_p) is taken as 0.6 from pore volume measurement and the liquid-phase diffusivity of hydrogen in GO solution is estimated using the Wilke−Chang equation.[36] At the GO hydrogenolysis conditions of this study, the value of the observable modulus ($\eta\varphi^2 = R_G \cdot (d_p/6)^2/(C_{H_2,S} \cdot D_{e,H_2} \cdot (1 - \varepsilon_B))$ ranges between 0.02 and 0.35, signifying that there are only minor mass transport resistances for hydrogen within the catalyst particles even at the conditions of most rapid reaction rate. First-order equivalent hydrogen intraparticle effectiveness factors are greater than 0.88 at those conditions, so we assume an intraparticle effectiveness factor for hydrogen of unity in all reactions.

For this system, the concentration profiles of GO and H_2 in and around the catalyst particles in a fully wetted trickle bed are represented in Figure 2. However, in our laboratory trickle-bed reactor liquid mass velocities are low under the operating conditions utilized, and the catalyst in the bed is only partially wetted.[30] To account for the effect of this partial wetting, we

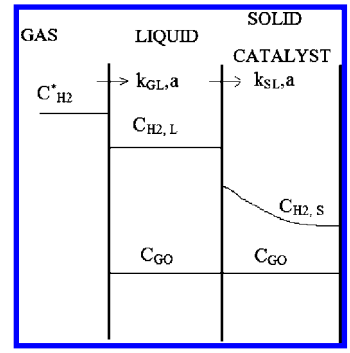

Figure 2. **Steady-state concentration profiles in the wetted fraction of the trickle-bed reactor.**

assume that reaction rate (R_G, mol GO/m^3 reactor/s) in the bed is a weighted summation of reaction rates occurring in the wetted and unwetted fractions of the trickle bed. In the wetted fraction (ε_W), mass transport resistances across the liquid film surrounding the catalyst particles must be accounted for as in Figure 2; hence, the reaction rate expression must include the hydrogen concentration at the catalyst surface ($C_{H_2,S}$), which is lower than that in the gas phase ($C^*_{H_2}$). In the unwetted fraction, there is no liquid layer surrounding the catalyst particle, and thus the hydrogen concentration at the catalyst surface is the same as in the gas phase ($C^*_{H_2}$). The reaction rate is thus given by

$$-R_G = \varepsilon_w(1 - \varepsilon_B)\frac{k_f C_{GO} C_{OH^-} C_{H_2,S}^2}{C_{GO} C_{OH^-} + K_H C_{H_2,S}^3} + (1 - \varepsilon_w)(1 - \varepsilon_B)\frac{k_f C_{GO} C_{OH^-} C_{H_2}^{*2}}{C_{GO} C_{OH^-} + K_H C_{H_2}^{*3}} \quad (11)$$

In this partial wetting scenario, the unwetted portion of the trickle bed can contribute an equal or greater share to overall reaction rate than the wetted portion, because there is no liquid layer to inhibit mass transport of hydrogen from gas to the catalyst particles in the unwetted region. To justify the existence of reactive liquid in the unwetted particles, it is assumed that the liquid phase in both wetted and unwetted fractions of the trickle bed is replenished continuously by the liquid phase continually changing its path down the bed, and thus reaction proceeds as described in eq 11.

While counterintuitive at first, the inclusion of reactive wetted and unwetted portions of the trickle bed is consistent with observations in actual trickle-bed operation[23] for gas-limited reactions, particularly when scaling up from laboratory to commercial systems. At the same space velocity, the higher liquid mass velocities in a large-scale trickle bed result in complete wetting and greater liquid film thicknesses, which in turn add resistance to mass transport of gaseous reactant to the catalyst and result in lower rates per unit catalyst volume. Partial wetting is considered further in the results presented later in this paper.

At steady state in the wetted fraction of the bed, hydrogen flux across gas−liquid and liquid−solid interfaces must equal the hydrogen consumption rate in the catalyst, resulting in the following relationships:

(35) Goto, S.; Smith, J. M. *AIChE J.* **1975**, *21*, 706–713.
(36) Wilke, C. R.; Chang, P. *AIChE J.* **1955**, *1*, 264–270.

$$k_{GL,H_2}a(C^*_{H_2} - C_{H_2,L}) = k_{SL,H_2}a(C_{H_2,L} - C_{H_2,S})$$

$$= (1 - \varepsilon_B)\frac{k_f C_{GO} C_{OH^-} C^2_{H_2,S}}{C_{GO}C_{OH^-} + K_H C^3_{H_2,S}} \quad (12)$$

These two algebraic equations are used to solve for the liquid and surface concentrations of hydrogen, $C_{H_2,L}$ and $C_{H_2,S}$, at each location in the reactor.

Solution Method. The GO molar balance and the trickle-bed energy balance equations were numerically integrated over the laboratory reactor length using Euler's method in a program written in Matlab 7.0. At each point along the reactor length, the hydrogen liquid-phase concentration ($C_{H_2,L}$) and surface hydrogen concentration ($C_{H_2,S}$) in the wetted bed fraction were determined from eq 12 by solving the linear and quartic equations, respectively, for each variable. Then reaction rate was calculated at that point, and the step to the subsequent point was taken. The number of steps ranged from 50 to 200 depending on reaction conditions; in all cases it was verified that step size was small enough to ensure that the solution obtained was unaffected by step size.

In the model equations, the wetted fraction of the trickle bed was taken from the correlation of Al-Dahhan et al.[16] Hydrogen partial pressure for each experiment was determined as the difference between total pressure and the partial pressure of water at the specified reaction temperature. Hydrogen concentration (solubility) in water (M) was calculated using a value of Henry's law constant of 120 MPa/(kmol/m^3) taken from the Linke compilation.[37] All other physical parameters were estimated from existing correlations;[38] values are given in Table 1.

Results

The reactor model was applied to a large set of steady-state trickle-bed reactor experiments at a variety of operating conditions (Table 2) to predict outlet GO conversion in each experiment. The strategy of the modeling exercise was to identify the set of kinetic parameters k_o, E_a, and K_H in the rate expression (eq 8) that minimizes the objective function defined in eq 13 below (essentially the sum over all 25 experiments of the square of the differences in square roots of the experimental and predicted GO outlet concentrations from the trickle-bed reactor). Because the reaction is only partial order in GO, this objective function, defined for a one-half order reaction, was found to lead to the best overall fit of the data at both low and high GO conversions. To help in the optimization, an initial value of activation energy E_a, calculated from batch reactor initial rate data, was used in order to facilitate more rapid error minimization.

$$\text{obj. function} = \sum_i (\sqrt{1 - X_{i,GO,exp}} - \sqrt{1 - X_{i,GO,cal}})^2 \quad (13)$$

Optimized values of the kinetic parameters are listed in Table 3. A comparison of experimental and predicted outlet GO conversions for all experiments is given in Table 2 and as a parity plot in Figure 3. In general, there is good agreement between predicted and experimental reactor performance—a remarkable outcome given that only the three kinetic constants are adjusted and all other constants and coefficients governing hydrodynamics and mass/heat transfer in the model are taken straight from literature or textbook correlations. For the optimized kinetic parameters, the value of the objective function in eq 13 is 0.123; in simplified terms, the average value of the absolute difference between experimental and simulated outlet GO conversion is 0.0455. This difference is independent of hydrogen pressure and reactor temperature over the ranges examined, but increases with increasing OH^- concentration. This systematic error could be remedied by inclusion of an additional kinetic parameter, such as an order "*n*" with respect to OH^- concentration in the numerator of eq 8, but there is no mechanistic basis for including such a parameter in the rate expression. We therefore accept the systematic error related to OH^- in light of maintaining the mechanistic basis and the fewest possible adjustable parameters in the rate expression.

An example of the experimental and predicted temperature profiles along the trickle bed at three different inlet temperatures is given in Figure 4; the model reasonably predicts the mild exotherms in the trickle-bed reactor over the temperature range examined. The model can also illustrate species concentration profiles in the trickle bed; Figure 5 gives predicted GO concentration profiles as a function of (a) inlet temperature, (b) liquid feed flow rate, and (c) feed base concentration at conditions that match those in the experiments identified. Figure 6 compares the experimental and predicted GO conversion on total reactor pressure; the sharp drop in conversion at the lowest pressure (2.76 MPa, exp 22) is attributed to low hydrogen partial pressure because water partial pressure at 463 K is 1.3 MPa, a significant fraction of the total. The observed drop in GO conversion as pressure increases above ~6 MPa is predicted by the mechanistically based rate expression.

If the rate expression (eq 8) with coefficients from Table 3 is evaluated at 463 K at the reactor inlet (C_{GO} = 4.6 M; C_{OH^-} = 0.28 M; P_{H_2} = 8.3 MPa) and normalized to the catalyst site

Table 1. **Physical properties (evaluated at 463 K) and reactor parameters for trickle-bed model**

description	unit	value
catalyst particle size (d_p)	m	0.0008
catalyst particle density	kg/m^3	1400
bed porosity (ε_B)		0.5
bed depth	m	0.27
reactor radius (R)	m	0.00635
liquid specific heat (C_p)	kJ/kg/K	4.18
liquid viscosity (μ_L)	kg/m/s	0.00014
liquid density (ρ_L)	kg/m^3	1100
gas viscosity (μ_g)	kg/m/s	1.38×10^{-5}
heat of reaction (ΔH_r)	kJ/kmol	−117,000
H_2 eff. liquid diffusivity (D_{e,H_2})	m^2/s	2.0×10^{-8}
liquid surface tension (σ)	kg/s^2	0.043

(37) Linke, William F. *Solubilities, Inorganic and Metal Organic Compounds: A Compilation of Solubility Data from the Periodical Literature*, 4th ed.; D. Van Nostrand: Princeton, NJ, 1958; Vol. 1.
(38) Perry, R. H.; Green, D. W.; Maloney, J. O. *Perry's Chemical Engineering Handbook*; McGraw-Hill: New York, 1997.

Table 2. **Summary of trickle-bed conditions and results**

exp. number	feed inlet temp (K)	total pressure (MPa)	feed flow rate (mL/h)	NaOH conc. (M)	experimental glycerol conversion	predicted glycerol conversion
1	468	8.27	50	0.58	0.90	0.97
2	464	8.27	50	0.58	0.95	0.98
3	467	8.27	50	0.28	0.81	0.84
4	464	8.27	50	0.14	0.69	0.55
5	475	8.27	50	0.14	0.83	0.75
6	453	8.27	50	0.14	0.46	0.38
7	463	8.27	35	0.14	0.79	0.67
8	463	8.27	25	0.14	0.86	0.81
9	473	8.27	35	0.14	0.87	0.85
10	473	8.27	35	0.14	0.89	0.85
11	453	8.27	50	0.28	0.65	0.58
12	475	8.27	50	0.28	0.94	0.95
13	463	8.27	35	0.28	0.89	0.90
14	463	8.27	25	0.28	0.94	0.97
15	453	8.27	35	0.28	0.75	0.72
16	473	8.27	35	0.28	0.96	0.99
17	453	8.27	25	0.28	0.79	0.85
18	473	8.27	25	0.28	0.98	1.00
19	463	8.27	35	0.28	0.91	0.90
20	463	11.03	35	0.28	0.88	0.83
21	463	5.52	35	0.28	0.91	0.96
22	463	2.76	35	0.28	0.64	0.60
23	463	13.79	35	0.28	0.82	0.79
24	468	13.79	35	0.28	0.91	0.87
25	468	8.27	35	0.28	0.96	0.96

Table 3. **Optimized kinetics parameters for rate expression (eq 8)**

description	unit	value
k_o	m^6 fluid/kmol/m^3 catalyst/s	8.26×10^{10}
E_a	kJ/kmol	86000
K_H	m^3/kmol	4.86×10^4

density of 1.3×10^{-5} kmol/kg, the resulting turnover frequency (TOF) is approximately 0.31 kmol H_2/kmol metal site/s. This is a reasonable value for GO hydrogenolysis at these conditions.

Evaluation of Model Assumptions

The trickle-bed model incorporates several significant features including a non-isothermal catalyst bed, mechanistically based intrinsic rate expression, multiple mass transfer resistances, and partial wetting of the catalyst in the trickle bed. Here we present simplifications of the original model that examine each of these assumptions to determine if their inclusion in the model is appropriate. The difference in value of the objective function given in eq 13 in the original and simplified models is used as a criterion for the validity of inclusion of each assumption in the model.

It is noted here that attempts were made to model glycerol hydrogenolysis with simple *n*th-order reaction kinetics in glycerol and hydrogen along with the mass transfer effects. None of these kinetic models gave a reasonably approximation of the experimental trickle-bed data. Thus, inclusion of the mechanistically based rate expression with the observed dependence on glycerol and hydrogen is an integral part of the modeling process.

Isothermal Catalyst Bed. The reactor energy balance (eq 10) is eliminated for an isothermal catalyst bed, as temperature is constant at the specified inlet value. The GO molar balance was integrated via Euler's method for all experiments, and the kinetic parameters k_o and K_H were reoptimized to minimize the objective function. The new optimized values are $K_H = 4.6 \times 10^4$ m^3/kmol and $k_o = 8.83 \times 10^{10}$ m^6 fluid/kmol/m^3 catalyst/s. With these optimal isothermal bed parameters, the value of the objective function (eq 13) for the isothermal trickle bed is 0.106, a value slightly smaller than the value of 0.123 obtained for the complete model. The average difference between predicted and experimental GO conversions for the isothermal model is 0.040 vs 0.045 for the complete model. Although the isothermal model thus appears to fit the GO conversion data slightly better than the complete model, the fact that it cannot predict temperature gradients in the trickle bed, which may be important in an expanded range of operation, makes it less attractive than the complete model.

It is possible that reactor temperature gradients measured experimentally (Figure 4) arise in part because of radial heat transfer resistances, which are not accounted for in the model. At this point, it is not possible to distinguish the effects of radial from axial temperature gradients because of limited measurement capabilities.

Fully Wetted Catalyst Bed. The low liquid velocities used in the experiments necessitate application of the partial wetting correlation of Al-Dahhan.[23] Here we examine the effect of fractional wetting (ε_W) of the catalyst bed on outlet conversion. First, the sensitivity of outlet GO conversion on fractional wetting was examined by varying ε_W from 50% to 200% of the value calculated by Al-Dahhan.[23] For outlet GO conversions above 85%, varying the fraction wetted changed the outlet conversion by a maximum of 10% (e.g., at a conversion of 85%, down to 77% for ε_W of twice its calculated value and up to 92% for ε_W of half its calculated value). At lower conversion values, the fraction wetted had a greater effect on overall GO conversion in the trickle bed, illustrating the importance of partial wetting in the trickle-bed process.

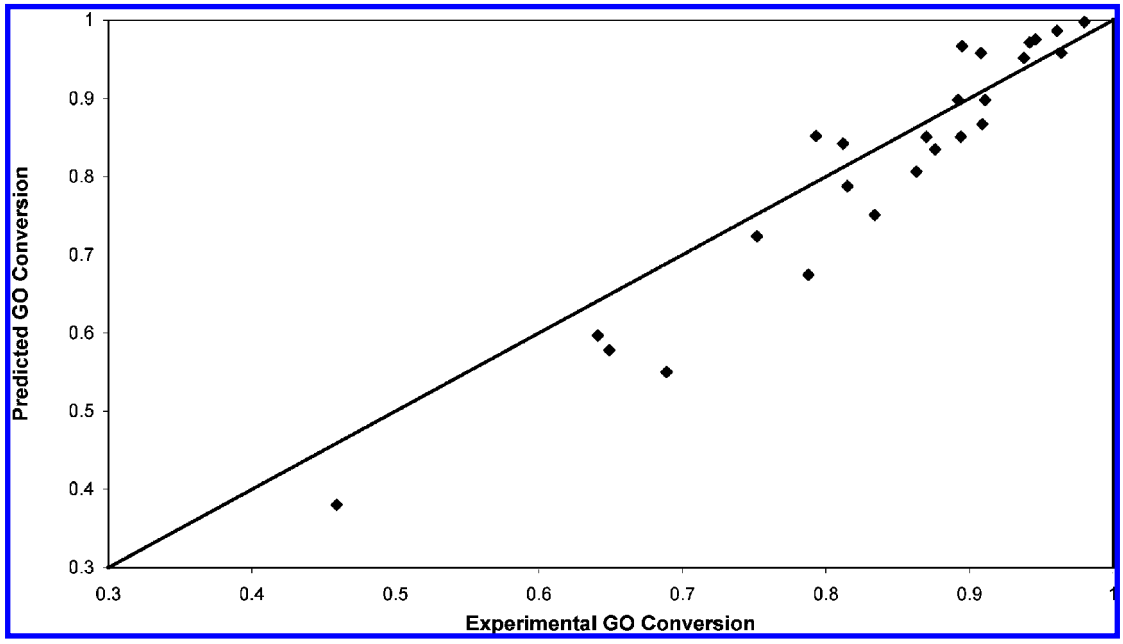

Figure 3. **Parity plot of experimental versus predicted GO conversion.**

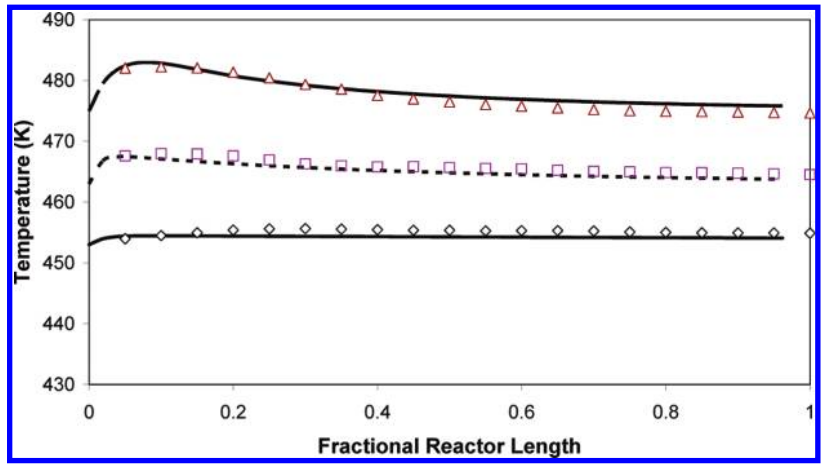

Figure 4. **Predicted vs experimental temperature profile in trickle bed. Inlet temperature: 453 K (exp 6): (—) - simulation, (◊) - experiment; 463 K (exp 7): (- - -) - simulation, (□) - experiment; 473 K (exp 9): (—) - simulation, (△) - experiment. Conditions: 8.27 MPa, liquid feed rate 35 mL/h, 0.14 M NaOH.**

To examine the extreme condition of a fully wetted bed, the overall rate expression (eq 11) is simplified to contain only the term for the wetted catalyst as shown below (eq 14).

$$-R_G = (1 - \varepsilon_B)\frac{k_f C_{GO} C_{OH^-} C_{H_2,S}^2}{C_{GO} C_{OH^-} + K_H C_{H_2,S}^3} \qquad (14)$$

This fully wetted bed rate expression was inserted into the reactor equations and the integration/optimization process was performed over all trickle-bed data. In this form, the fully wetted particle model significantly underpredicts outlet GO concentration from the trickle bed at all but the highest pressure (13.8 MPa) investigated. At the lower pressures, gas−liquid mass transfer resistance limits the overall reaction rate in the fully wetted bed, and the maximum possible reaction rate thus becomes the maximum gas−liquid mass transfer rate in the bed: $R_{GL,\ max} = k_{GL,H_2} a C_{H_2}^*$. Assuming this value as constant throughout the trickle bed, the maximum possible GO conversion is about 57% at 8.3 MPa pressure (7.5 MPa H_2 pressure), well below the values obtained experimentally. At the highest pressure (13.8 MPa, runs 23 and 24), the predicted conversions are close to the experimental values, suggesting that the reaction is moving away from being hydrogen mass transfer limited in the wetted fraction at high pressures. Overall, however, the conclusion must be drawn that the unwetted portion of the catalyst bed contributes significantly to reaction rate. It is possible that the actual value of the gas−liquid mass transfer coefficient is significantly larger than that predicted by the correlation of Goto and Smith, and thus the bed could be nearly fully wetted and giving the observed conversions; however, that notion is inconsistent with the literature and the correlations used for both wetting and mass transfer.[34]

Further, the substantial body of literature on trickle-bed reactors[15−23] clearly indicates that partial wetting of the catalyst bed plays a significant role in determining trickle-bed behavior

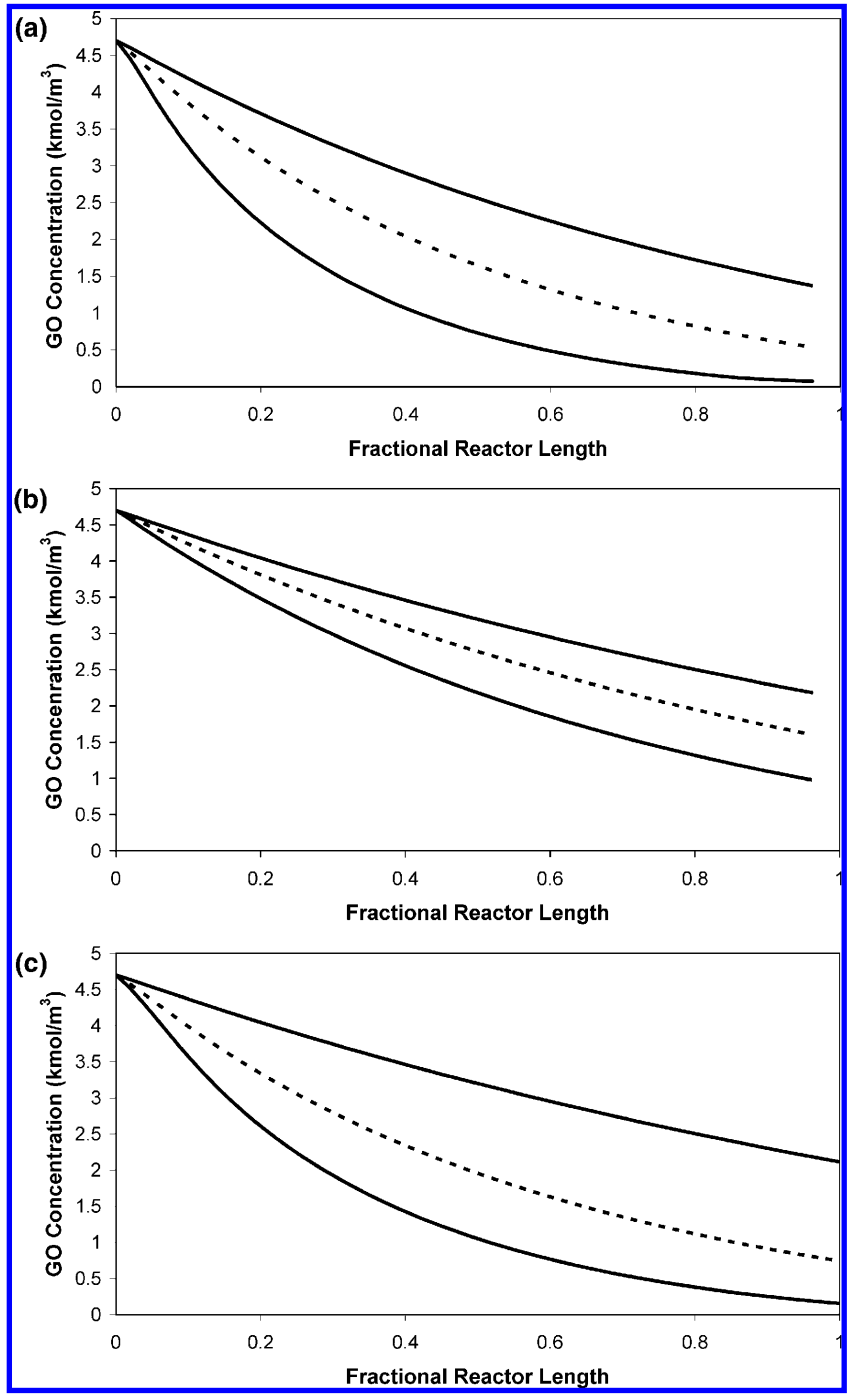

Figure 5. **(a) Simulated GO concentration profiles in trickle bed for different inlet temperatures. (—) - 453 K (exp 15); (- - -) - 463 K (exp 13); (—) - 473 K (exp 16). Conditions: 8.27 MPa, liquid feed rate 35 mL/h, 0.28 M NaOH. (b) Simulated GO concentration profiles in trickle bed for different liquid feed flow rates: (—) - 50 mL/h (exp 4); (- - -) - 35 mL/h (exp 7); (—) - 25 mL/h (exp 8). Conditions: 8.27 MPa, 463 K, 0.14 M NaOH. (c) Simulated GO concentration profiles in trickle-bed reactor at different NaOH concentrations: (—) - 0.58 M (exp 2); (- - -) - 0.28 M (exp 3); (—) - 0.14 M (exp 4). Conditions: 8.27 MPa, 464 K, liquid feed rate 50 mL/h.**

at low-flow conditions. The question of how the unwetted portion of a trickle-bed reactor contributes to reaction, as assumed here, seems difficult at first to reconcile. We make the assumption that the pore volume of all catalyst particles in the bed are filled with liquid and that the bulk liquid flowing over part of the catalyst is continuously changing its path along the trickle bed. Thus, while only a portion of the catalyst is wetted at any instant, the particular portion wetted changes continuously. When catalyst particles are wetted, the liquid inside them exchanges reactants and products with the bulk liquid, hence facilitating reaction when again unwetted. This continuous liquid replenishing of the unwetted region from bulk liquid appears a reasonable first approximation of characterizing partial wetted trickle beds and avoids the major challenges associated with attempting to model bed hydrodynamics.

Gas−Liquid Mass Transfer Coefficient Sensitivity Analysis. The hydrogen gas−liquid mass transfer coefficient k_{GL,H_2} from the correlation of Goto and Smith[34] was varied from 50%

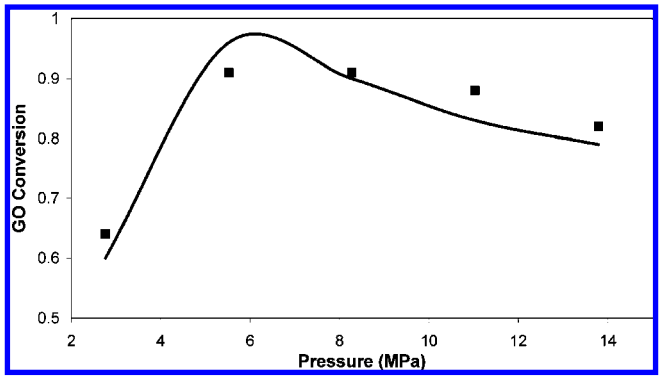

Figure 6. **Effect of pressure on outlet GO conversion from trickle-bed reactor. (—) - simulation; (■) - experiment. Conditions: 463 K, liquid feed rate 35 mL/h, 0.28 M NaOH.**

to 200% of its calculated value and inserted into the partial wetted trickle-bed model. Over the full range of experimental conditions, the outlet GO conversion varied by less than five percentage points over the range of k_{GL-H_2} investigated. This outcome is partially explained by the fact that the reaction rate (eq 8) is weakly or even negatively dependent on hydrogen concentration ($C_{H_2,S}$) at the catalyst particle and also by the fact that the unwetted portion of the trickle bed makes a substantial contribution to overall reaction rate.

Conclusions

Experimental data of GO hydrogenolysis in a laboratory-scale trickle-bed reactor have been described with a one-dimensional, non-isothermal trickle-bed reactor model involving a mechanistically based kinetic rate expression, intraparticle mass transport, interphase mass transport, and partial wetting of the catalyst bed. The model is fit to the experimental data by optimizing values of the kinetic constants in the rate expression. The rate expression predicts rate dependencies on GO and H_2 that vary significantly in order, depending on particular experimental conditions, indicating that the interplay between mass transport resistances, fractional wetting of catalyst, and observed reaction rate is complex. Axial temperature gradients are small (<10 °C) yet play a role in the trickle bed, and the unwetted portion of the bed contributes significantly to overall reaction rate. Accounting for all complexities and assumptions, the model reasonably predicts the outlet conversion of GO from the trickle bed.

Acknowledgment

This work was supported by funding from the U.S. Department of Energy, Office of the Biomass Program, to Pacific Northwest National Laboratory (PNNL), a multiprogram national laboratory operated by Battelle for the U.S. Department of Energy under Contract DE-AC06-76RL01830. Michigan State University acknowledges the support of Pacific Northwest National Laboratory for their part of the work. We thank Alan Zacher for thoughtful contributions in reviewing this manuscript prior to submission.

NOMENCLATURE

$C_{GA\cdot S}$	adsorbed glyceraldehyde intermediate concentration (kmol/m^3 fluid)
C_{GO}	glycerol concentration (kmol/m^3 fluid)
C_{H_2}	hydrogen concentration in liquid (kmol/m^3 fluid)
$C^*_{H_2}$	liquid phase concentration of hydrogen in equilibrium with gas phase (kmol/m^3 fluid)
$C_{H_2,L}$	hydrogen concentration in bulk liquid phase (kmol/m^3 fluid)
$C_{H_2,S}$	hydrogen liquid phase concentration at catalyst surface (kmol/m^3 fluid)
$C_{I\cdot S}$	adsorbed intermediate concentration (kmol/m^3 fluid)
C_{OH^-}	base concentration (kmol/m^3 fluid)
C_p	specific heat of solution (kJ/kg/K)
C_S	vacant site concentration on catalyst surface (kmol/m^3 fluid)
C_{total}	total site concentration on catalyst surface (kmol/m^3 fluid)
d_p	catalyst particle diameter (m)
D_{e,H_2}	hydrogen effective diffusivity (m^3 fluid/m cat/s)
E_a	activation energy in k_f (kJ/kmol)
ΔH_R	heat of reaction (kJ/kmol)
k_f	rate constant (m^6 fluid/kmol/m^3 catalyst/s)
$k_{GL,H_2}a$	hydrogen gas−liquid interfacial mass transfer coefficient (m^3 fluid/m^3 reactor/s)
k_0	pre-exponential coefficient of k_f (m^6 fluid/kmol/m^3 catalyst/s)
$k_{SL,H_2}a$	hydrogen solid−liquid interfacial mass transfer coefficient (m^3 fluid/m^3 reactor/s)
K_H	constant in rate expression (m^3/kmol)
k_1, k_{-1}	dehydrogenation rate constants (m^6/m^3 catalyst/kmol/s)
k_2, k_{-2}	dehydration rate constants (m^6/m^3 catalyst/kmol/s)
k_3	hydrogenation rate constant (m^9/m^3 catalyst/kmol^2/s)
r_1	dehydrogenation rate (kmol/m^3 catalyst/s)
r_2	dehydration rate (kmol/m^3 catalyst/s)
r_3	hydrogenation rate (kmol/m^3 catalyst/s)
R	reactor radius (m)
R_G	observed (global) consumption rate of hydrogen and glycerol (kmol/m^3 reactor/s)
t	time (s)
T	temperature (K)
T_c	coolant jacket temperature (K)
U_o	overall heat transfer coefficient, J/m^2/K/s
X_{GO}	glycerol conversion at trickle bed outlet
ε_W	fraction of bed wetted
ε_B	bed porosity (m^3 void/m^3 reactor)
ρ	fluid density (kg/m^3)
τ	trickle bed residence time (m^3 reactor·s/m^3 fluid)

Supporting Information Available

This material is available free of charge via the Internet at http://pubs.acs.org.

Received for review December 22, 2009.

OP900336A